

Analysis of Low-Energy K^+p Scattering Data by a New Method

R. E. CUTKOSKY* AND B. B. DEO†

Physics Department, Carnegie-Mellon University, Pittsburgh, Pennsylvania 15213

(Received 5 September 1969)

A new method, recently devised by us, is used for the analysis of K^+p scattering data below 1.5 GeV/c. This analysis uses, instead of the ordinary partial-wave expansion, a method of expansion with optimally accelerated convergence properties; the method has been devised by the use of analytic approximation theory. Although no experimental information is used which was not available to Lea, Martin, and Oades, somewhat more definite results are obtained by the present method. The results are sensitive to the values assumed for the coupling constants $g_{KN\Lambda}$ and $g_{KN\Sigma}$; the results appear to be most consistent if values close to the SU_3 prediction are used for these coupling constants. With the use of the SU_3 prediction, rather strong P -wave scattering is found in the low-energy region.

I. INTRODUCTION

DATA on low-energy K^+p elastic scattering have been analyzed by Lea, Martin, and Oades (LMO).¹ We present here a reanalysis of many of the same data, using a new method recently devised by us.² Our approach differs from that of LMO in several respects. We have not attempted to make an energy-dependent analysis at momenta higher than 650 MeV/c, but we just try to link up the phase-shift solutions found at each energy through separate analyses. However, the principal difference is that we represent the scattering amplitude in a different way; in fact, the main purpose of this work is to illustrate the application of this new method in a practical situation. We parametrize the scattering amplitude according to an optimally convergent method, which accommodates the correlations among the partial-wave amplitudes which are required by the momentum-transfer analyticity properties. The parametrization of the inelastic part of the amplitude is especially different from that of LMO, because we do not need to make any special assumptions about which partial waves are responsible for the production processes. The correlations among the partial-wave amplitudes which we have exploited arise, ultimately, from the fact that the forces between the particles depend smoothly on the distance (because these forces are produced by exchange of other particles) and have a definite range (because the exchanged particles have known masses). Our approach, however, is otherwise model independent; we do not need to assume that the forces have any special features, apart from the forces which are associated with the so-called pole terms, which are relatively unambiguous.

Our results are, in general, similar to those of LMO; at most energies, however, we found only two distinct sets of phase shifts which were consistent with the angular distribution, which is many fewer than they found. Moreover, with use of the limited polarization data available at the time we began this work, or with use of data on K^+n charge-exchange scattering,³ a unique set of phase shifts was found at low momenta. For this set, the P waves are more important than in the LMO fits. Unfortunately, the statistical accuracy of the data is, in general, rather low, and, as a result, the phase shifts have large uncertainties. The phase shifts, as a function of energy, are really only determined to lie within very broad bands. As LMO had already emphasized, polarization data in the 1000–1500 MeV/c region are essential for determination of the trend of the phase shifts in this region, and, in particular, for ascertaining whether the $P_{1/2}$ partial wave resonates. The data of Andersson *et al.*⁴ ruled out the resonant possibility; these data became available as we completed our analysis.

We have defined the polarization according to the same convention as LMO.

II. PARAMETRIZATION OF SCATTERING AMPLITUDE

Electromagnetic corrections were taken into account by us in the same approximation used by LMO. With neglect of the electromagnetic interactions, the two invariant amplitudes conventionally denoted by $A(s, t)$ and $B(s, t)$ are free of kinematical singularities and (for fixed s) are supposed to be analytic for t in a cut plane. (Here s , t , and u are the Mandelstam variables.) There are poles at $u = M_\Lambda^2$ and $u = M_\Sigma^2$, and branch cuts for $u \geq (M_\Lambda + M_\pi)^2$ and $t \geq 4M_\pi^2$. We have shown² that the most rapidly convergent polynomial expansion is obtained by mapping the cut plane of $x = \cos\theta$ onto the interior of a unifocal ellipse,

* On leave at the Department of Applied Mathematics and Theoretical Physics, University of Cambridge, Cambridge, England (1968–69).

† Now at Department of Physics, Utkal University, Orissa, India.

¹ A. T. Lea, B. R. Martin, and G. C. Oades, *Phys. Rev.* **165**, 1770 (1968).

² R. E. Cutkosky and B. B. Deo, *Phys. Rev.* **174**, 1859 (1968).

³ A. K. Ray, R. W. Burris, H. E. Fisk, R. W. Kraemer, D. G. Hill, and M. Sakitt, *Phys. Rev.* **183**, 1183 (1969).

⁴ S. Andersson, C. Daum, F. C. Erne, J. P. Lagnaux, J. C. Sens, and F. Udo, *Phys. Letters* **28B**, 611 (1969).

in which the physical region $-1 \leq x \leq 1$ is mapped onto the line segment $-1 \leq z \leq 1$, and the branch cuts are mapped onto the ellipse. A similar method has been suggested by Ciulli.⁵ Some additional refinements have been subsequently developed by one of us⁶ but are not used in this work.

The pole terms in A or B are introduced explicitly, and the remainders are then represented by polynomial expansions in z . Actually, as pointed out in Ref. 2, it is of great advantage, especially at low momenta, to exploit the fact that the imaginary parts of A and B are analytic in a large region of the x plane, and to use separate transformations and expansions for the real and imaginary parts. The branch points of the imaginary parts are obtained from the Landau curves for certain well-known "box" diagrams.

Note that, at energies somewhat above threshold, the leading singularities of the imaginary part are associated with inelastic processes.

In Ref. 2 we discussed at some length how to make unitarity approximations for the case of spinless particles. In the present case, it is only necessary to extend the notation slightly, in order to accommodate the fact that there are two amplitudes and two sets of partial waves, with $j = l \pm \frac{1}{2}$. Let us denote the partial-wave amplitudes as

$$a_m = x_m + i\dot{y}_m, \quad (1)$$

where the index is

$$m = j + l + \frac{1}{2}. \quad (2)$$

We write the scattering amplitude in the form

$$F(x) = f_1(x) + \sigma \cdot \hat{\kappa}' \sigma \cdot \hat{\kappa} f_2(x), \quad (3)$$

where $\hat{\kappa}$ and $\hat{\kappa}'$ are unit vectors in the directions of the initial and final kaon momenta. The amplitudes f_i are linear combinations of A and B , with coefficients which depend only on the energy. We now expand the real parts of the f_i (apart from the contribution of the pole terms) in polynomials in z . Let ξ_n , with $n = i + 2r$, be the coefficient of z^r in f_i , and let the total number of coefficients be N , where N is any positive integer. The order of the approximation is defined by N , which determines where the two expansions are truncated.

Following the method of Ref. 2, we construct all of the x_m from the polynomial approximations to the f_i by the usual integration formula, leading to equations of the form

$$x_m = \sum_{n=1}^N C_{mn} \xi_n + X_m, \quad (4)$$

where the X_m are the "Born approximation" (the contribution of the Λ and Σ poles). In general, none

of the x_m would vanish, but we would expect that the amplitudes with lowest angular momenta would be related most directly to the coefficients. Given the x_m for $m = 1, \dots, N$, we may calculate the coefficients by solving (4):

$$\xi_n = \sum_{m=1}^N D_{Nnm} (x_m - X_m). \quad (5)$$

On substituting back into (4), we obtain

$$\hat{x}_m = \sum_{n=1}^N \Gamma_{Nnm} (x_n - X_n) + X_m, \quad (6)$$

where

$$\Gamma_{Nmn} = \sum_k C_{mk} D_{Nkn}. \quad (7)$$

We have put a caret on the variable on the left-hand side of (6) because it is just an approximation for $m > N$, as we shall describe shortly. The imaginary parts of the partial-wave amplitudes, y_m , are given by formulas exactly like (6), except that there is no Born approximation, and the values of the coefficients Γ_{Nmn} are somewhat different, because of the different domain of analyticity of the imaginary parts of the f_i .

We have, through Eq. (6) and its counterpart for y_m , parametrized the set of partial-wave amplitudes by the values of the first N . For $m \leq N$, therefore, we can guarantee explicitly that the partial waves satisfy the unitarity condition. However, for $m > N$, the amplitude $\hat{a}_m = \hat{x}_m + i\dot{y}_m$ will not, in general, be unitary. We define the unitarized amplitude a_m to be the amplitude, satisfying the unitary condition, obtained by adding to \hat{a}_m the complex number of smallest possible modulus. In the study reported here, we found that in all cases only very small corrections needed to be made for unitarity, provided SU_3 values were used for the coupling constants, and when the total inelastic cross section was appreciable, no correction was needed—the inelasticity of all partial waves was positive. This result is related to the fact that the inelastic processes controlled the rate of convergence of the imaginary part. In other words, the fact that our expansion does not satisfy elastic unitarity term by term is an advantage, rather than a defect.

The computational procedure used in the present study was as follows. At each momentum, we first calculated the elliptic mapping, using the algorithm described in Ref. 2, for about 400 points in the physical region. The C_{mn} and X_m were then computed by numerical integration. In calculating the X_m , we neglected the Λ - Σ mass difference and used the form factor described in earlier work.⁷ The X_m and the Γ_{Nmn} for both the real and imaginary parts were then punched on cards. In the data-fitting program, the a_m for $m \leq N$ were considered as parameters; from them the \hat{a}_m were calculated and unitarized as described above, and then the partial-wave sum was evaluated.

⁵ S. Ciulli, Nuovo Cimento **61A**, 787 (1969).

⁶ R. E. Cutkosky, Ann. Phys. (N.Y.) **54**, 350 (1969).

⁷ R. E. Cutkosky and B. B. Deo, Phys. Rev. Letters **20**, 1272 (1968).

In order to understand the practical effect of the expansion, it is useful to note that the Γ 's possess the following properties:

(i) By construction,

$$\Gamma_{Nmn} = \delta_{mn} \quad \text{for } m, n \leq N.$$

(ii) At low momenta ($p \rightarrow 0$),

$$\Gamma_{Nmn} \rightarrow 0 \quad \text{for } m > N$$

(unless N is even, $n=N$ and $m=N+1$).

(iii) For $m > N+1$, we have the consistency relation

$$\Gamma_{N+1,mn} + \Gamma_{N+1,m,N+1} \Gamma_{N,N+1,n} = \Gamma_{Nmn}.$$

This means that if the \hat{a}_m are first obtained from the a_n for $n \leq N$ using the Γ_{Nmn} , then if we use \hat{a}_{N+1} as a given parameter and construct the \hat{a}_m ($m > N+1$) using the $\Gamma_{N+1,mn}$, we get the same values as before; in other words, the higher partial waves are stable in a change of N .

(iv) Since the constant terms in f_1 and f_2 contribute only to $S_{1/2}$ and $P_{1/2}$, or, in other words,

$$C_{mn} = \delta_{mn} \quad \text{if } n = 1, 2,$$

we have also

$$D_{Nmn} = \delta_{mn} \quad \text{if } n = 1, 2,$$

and therefore

$$\Gamma_{Nmn} = \delta_{nm} \quad \text{if } m = 1, 2.$$

This means that the $S_{1/2}$ and $P_{1/2}$ amplitudes are not correlated with the higher partial waves. In particular, the Born approximation to the $S_{1/2}$ and $P_{1/2}$ amplitudes is of no consequence in the partial wave analysis. The elliptical transformation does not have much effect, therefore, if the $S_{1/2}$ and $P_{1/2}$ amplitudes dominate in the Born approximation as well as in the physical amplitude or in other words, if purely short-range effects predominate. On the other hand, the higher partial-wave amplitudes are correlated with the $P_{3/2}$ or $D_{3/2}$ amplitudes, for example. Furthermore, since the form factor used in the Born approximation mainly affects the $j = \frac{1}{2}$ amplitudes, the results are not very sensitive to the choice of this form factor.

It is usually assumed that the phase shifts with the same value of l are of similar importance, and that the partial wave sum should be truncated with the terms $l = l_{\max}$; then $f_2(x)$ is a polynomial in x which is one degree lower than $f_1(x)$. Our truncation, when N is odd, is similar in spirit. However, we do not know any convincing general argument why the total angular momentum should always be less significant than the orbital angular momentum. In some cases, although not, perhaps, at very low energies, it might be reasonable to include terms of the same order in f_1 and f_2 . We have therefore also allowed for truncations with even values of N . In either case, of

course, the point of truncation should be determined by consideration of the convergence rate of the expansions and the statistical significance of the parameters.⁶ In the present initial study, we have primarily used the minimum number of parameters needed for a reasonable value of χ^2 . However, we have also been guided by the numbers of parameters needed at nearby energies, and the estimated uncertainties are based on a conservatively large number of parameters.

III. DATA

We have used the following subset of the data discussed by LMO. These data are the differential cross section only, unless otherwise noted.

(i) 140–642 MeV/ c (combined): Data of Goldhaber *et al.*⁸

(ii) 520 MeV/ c : Data of Ref. 8, combined with the data of Kycia *et al.*,⁹ which were renormalized by 10% as suggested by LMO.

(iii) 642 MeV/ c : Ref. 8.

(iv) 778 MeV/ c : Differential cross section data of Focardi *et al.*¹⁰ and polarization data (two points) of Femino *et al.*¹¹

(v) 860 MeV/ c : Unpublished data of Bland *et al.*¹²

(vi) 910 MeV/ c : Differential cross section data and polarization data (four points) of Hirsch and Gidal.¹³

(vii) 960 MeV/ c : Ref. 12.

(viii) 1170 MeV/ c : Cook *et al.*¹⁴

(ix) 1200 MeV/ c : Carroll *et al.*¹⁵ and Ref. 12.

(x) 1450 MeV/ c : Bettini *et al.*¹⁶

The data most useful for our purposes appeared to be (i), (iv), (vi), (viii), and (x). Although the polarization data of (iv) and (vi) had very poor statistics, these polarization data did help to delimit the phase shifts; the angular distribution at 778 MeV/ c had the better statistics. The data (x) had good statistics, but the energy may be too high for the small number of parameters we used. (We got reasonable fits, but good polarization data or a careful

⁸ S. Goldhaber, W. Chinowsky, G. Goldhaber, W. Lee, T. O'Halloran, T. F. Stubbs, G. M. Pjerrou, D. H. Stork, and H. K. Ticho, *Phys. Rev. Letters* **9**, 135 (1962).

⁹ T. F. Kycia, L. T. Kerth, and R. G. Baender, *Phys. Rev.* **118**, 553 (1960).

¹⁰ S. Focardi, A. Minguzzo-Ranzi, L. Monari, G. Saltini, and P. Serra, *Phys. Letters* **24B**, 314 (1967).

¹¹ S. Femino, S. Jannelli, and F. Mezzanares, *Nuovo Cimento* **50A**, 371 (1967).

¹² R. W. Bland *et al.*, quoted by G. Goldhaber, in UCRL-Report No. UCRL-17388 (unpublished).

¹³ W. Hirsch and G. Gidal, *Phys. Rev.* **135**, B191 (1964).

¹⁴ V. Cook, D. Keefe, L. T. Kerth, P. G. Murphy, W. A. Wenzel, and T. F. Zipf, *Phys. Rev.* **129**, 2743 (1963).

¹⁵ A. S. Carroll, J. Fischer, A. Lundby, R. H. Phillips, C. L. Wang, F. Lobkowitz, A. C. Melissinos, Y. Nagashima, C. A. Smith, and S. Tewksbury, *Phys. Rev. Letters* **21**, 1282 (1968).

¹⁶ A. Bettini, M. Cresti, S. Limentari, L. Peruzzo, R. Santangelo, D. Locke, D. J. Crennell, W. T. Davies, and P. B. Jones, *Phys. Letters* **16**, 83 (1965).

TABLE I. Values of the phase shifts (in degrees) for various laboratory momenta (in MeV/c) and coupling constants, obtained in the energy-dependent fit to the lower-energy data.

g^2	P (lab) P_j	140 $N=7$	175 7	205 7	235 7	265 7	355 6	520 6	642 6	χ^2 (49)
(F)										
0	$-\frac{1}{2}$	-7.8	-9.8	-11.5	-13.2	-15.0	-20.1	-29.0	-34.8	53.5
	$+\frac{1}{2}$	-0.05	-0.10	-0.15	-0.23	-0.32	-0.73	-2.0	-3.4	
	$+\frac{3}{2}$	0.04	0.07	0.11	0.17	0.24	0.53	1.5	2.5	
	$-\frac{3}{2}$	0.001	0.003	0.007	0.012	0.020	0.060	0.22	0.41	
	$-\frac{5}{2}$	0.001	0.003	0.007	0.012	0.020	0.060	0.22	0.41	
	(χ^2)	2.3	7.8	15.1	7.4	2.9	8.1	2.8	7.1	
7	$-\frac{1}{2}$	-7.7	-9.6	-11.4	-13.1	-14.8	-19.9	-28.7	-34.5	52.0
	$+\frac{1}{2}$	-0.10	-0.19	-0.30	-0.44	-0.62	-1.4	-3.9	-6.6	
	$+\frac{3}{2}$	+0.06	+0.12	0.19	0.28	0.40	0.90	2.5	4.2	
	$-\frac{3}{2}$	-0.000	-0.000	-0.001	-0.002	-0.002	1.002	0.06	0.17	
	$-\frac{5}{2}$	-0.001	-0.002	-0.004	-0.008	-0.012	-0.036	-0.17	-0.18	
	(χ^2)	2.2	8.3	14.7	7.2	2.7	8.3	4.5	4.1	
14	$-\frac{1}{2}$	-7.8	-9.8	-11.4	-13.1	-14.8	-19.6	-27.6	-32.7	52.8
	$+\frac{1}{2}$	-0.15	-0.30	-0.47	-0.69	-0.98	-2.2	-6.1	-10.3	
	$+\frac{3}{2}$	0.09	0.18	0.29	0.43	0.60	1.4	3.8	6.4	
	$-\frac{3}{2}$	-0.002	-0.004	-0.008	-0.013	-0.02	-0.05	-0.07	-0.01	
	$-\frac{5}{2}$	-0.003	-0.007	-0.015	-0.026	-0.04	-0.12	-0.41	-0.70	
	(χ^2)	2.2	7.6	15.0	6.9	2.7	8.5	5.8	4.5	
21	$-\frac{1}{2}$	-7.9	-9.9	-11.5	-13.1	-14.7	-19.2	-26.5	-31.1	55.6
	$+\frac{1}{2}$	-0.20	-0.38	-0.60	-0.88	-1.2	-2.8	-7.7	-13.0	
	$+\frac{3}{2}$	0.12	0.22	0.35	0.55	0.74	1.7	4.6	7.7	
	$-\frac{3}{2}$	-0.003	-0.009	-0.02	-0.03	-0.04	-0.11	-0.26	-0.31	
	$-\frac{5}{2}$	-0.005	-0.014	-0.03	-0.05	-0.08	-0.23	-0.76	-1.4	
	(χ^2)	2.2	6.9	15.5	7.0	2.8	9.4	7.9	3.9	
(Y)										
0	$-\frac{1}{2}$	-7.8	-9.6	-11.4	-13.1	-14.8	-19.9	-28.7	-34.5	53.0
	$+\frac{1}{2}$	0.12	0.24	0.37	0.55	0.78	1.8	4.8	8.2	
	$+\frac{3}{2}$	-0.05	-0.09	-0.14	-0.21	-0.29	-0.66	-1.8	-3.1	
	$-\frac{3}{2}$	-0.002	-0.004	-0.009	-0.015	-0.025	-0.074	-0.27	-0.50	
	$-\frac{5}{2}$	-0.002	-0.004	-0.009	-0.015	-0.025	-0.074	-0.27	-0.50	
	(χ^2)	2.0	8.3	14.7	7.0	2.7	9.0	7.1	2.2	
7	$-\frac{1}{2}$	-7.7	-9.7	-11.4	-13.1	-14.8	-20.0	-28.8	-34.6	64.6
	$+\frac{1}{2}$	0.12	0.23	0.37	0.55	0.77	1.8	4.8	8.1	
	$+\frac{3}{2}$	-0.04	-0.08	-0.13	-0.20	-0.28	-0.63	-1.7	-3.0	
	$-\frac{3}{2}$	-0.004	-0.01	-0.02	-0.04	-0.06	-0.17	-0.57	-1.0	
	$-\frac{5}{2}$	-0.005	-0.01	-0.02	-0.04	-0.07	-0.21	-0.74	-1.3	
	(χ^2)	2.3	9.1	14.3	6.9	2.8	11.8	13.9	3.5	
14	$-\frac{1}{2}$	-8.2	-10.1	-11.6	-13.2	-14.6	-18.6	-24.8	-28.5	72.9
	$+\frac{1}{2}$	0.29	0.55	0.88	1.3	1.8	4.1	11.3	18.8	
	$+\frac{3}{2}$	-0.10	-0.19	-0.31	-0.45	-0.64	-1.4	-4.0	-6.8	
	$-\frac{3}{2}$	-0.008	-0.02	-0.04	-0.08	-0.12	-0.36	-1.2	-2.1	
	$-\frac{5}{2}$	-0.01	-0.03	-0.05	-0.09	-0.15	-0.44	-1.5	-2.8	
	(χ^2)	2.7	6.1	15.4	6.5	2.6	14.2	19.9	5.5	
21	$-\frac{1}{2}$	-8.4	-10.2	-11.7	-13.1	-14.5	-18.1	-23.3	-26.4	91.0
	$+\frac{1}{2}$	0.33	0.63	1.0	1.5	2.1	4.7	12.8	21.1	
	$+\frac{3}{2}$	-0.11	-0.21	-0.34	-0.50	-0.70	-1.6	-4.4	-7.4	
	$-\frac{3}{2}$	-0.01	-0.03	-0.06	-0.10	-0.16	-0.47	-1.6	-2.8	
	$-\frac{5}{2}$	-0.01	-0.04	-0.07	-0.12	-0.20	-0.59	-2.1	-3.7	
	(χ^2)	3.8	5.5	15.8	6.3	2.9	19.3	26.8	10.6	

TABLE II. The scattering lengths and the S -wave effective ranges as obtained from the acceptable fits to the lower-energy data.

g^2	a_s	r_{0s}	$a_{p1/2}$	$a_{p3/2}$
0 (Y)	-0.283 ± 0.004	0.54 ± 0.09	0.020 ± 0.005	-0.008 ± 0.002
0 (F)	-0.286 ± 0.004	0.54 ± 0.09	-0.009 ± 0.004	0.006 ± 0.002
7	-0.283 ± 0.006	0.54 ± 0.09	-0.018 ± 0.005	0.011 ± 0.002
14	-0.292 ± 0.006	0.35 ± 0.09	-0.028 ± 0.003	0.016 ± 0.001
21	-0.299 ± 0.005	0.15 ± 0.10	-0.038 ± 0.006	0.021 ± 0.004

study of the energy dependence might show a need for more parameters.)

In polynomial fits to the differential cross section, for the purpose of estimating the coupling constant⁷ $g_{\Lambda\Sigma^2} = g_{KNA^2} + g_{KN\Sigma^2}$ and the real part of the forward scattering amplitude,¹⁷ reasonably precise ($\pm 35\%$) and consistent estimates of $g_{\Lambda\Sigma^2}$ were obtained from the data (iv), (vii), and (viii). The data (v) seemed to give too large a value ($g_{\Lambda\Sigma^2} = 22 \pm 6$); this may be related to the fact that the backward points of (v) do not appear to lie on LMO's interpolated curve. The values of $g_{\Lambda\Sigma^2}$ adduced from (ix) and (x) were somewhat low and had very large uncertainties. The consistency of the two sets of angular distributions of (ix) with each other or with (viii) appeared to be marginal. It has since been reported¹⁸ that systematic errors have been found in the data (ix).

The data (ii) and (iii) have limited statistical accuracy for a fixed-energy analysis and are really at too-low momenta for our transformation to have a pronounced effect. We included them in our analysis in order to provide a basis for comparison with the K^+d charge-exchange scattering experiment at 600 MeV/c of Ray *et al.*³ In addition, these data were used in an energy-dependent analysis.

At all energies, we used as additional input data values of the forward amplitude as obtained from the dispersion-relation studies of Martin and Poole¹⁹ and Lusignoli *et al.*²⁰ We also used the total cross-section data of Cool *et al.*²¹

TABLE III. The phase shifts (in degrees) at 600 MeV/c, obtained from our best fit, compared with the values obtained by Ray *et al.* from a standard analysis which included charge-exchange data.

P_j	$-\frac{1}{2}$	$+\frac{1}{2}$	$+\frac{3}{2}$
This work, $g^2=14$	-31	-8.5	5.3
Reference 3	-32.7 ± 3.0	-8.6 ± 3.0	4.2 ± 3.0

¹⁷ Y. A. Chao, R. E. Cutkosky, and B. B. Deo, in *Proceedings of the Fourteenth International Conference on High-Energy Physics, Vienna, 1968* (CERN, Geneva, 1969).

¹⁸ R. Levi Setti, Rapporteur, Proceedings of the Lund International conference on Elementary Particles (1969) (unpublished), p. 340.

¹⁹ A. D. Martin and F. Poole, Nucl. Phys. **B4**, 467 (1968).

²⁰ M. Lusignoli, M. Restignoli, G. A. Snow, and G. Violini, Phys. Letters **21**, 229 (1966).

²¹ R. L. Cool, G. Giacomelli, T. F. Kycia, B. A. Leontic, K. K. Li, A. Lundley, and J. Teiger, Phys. Rev. Letters **17**, 102 (1966).

IV. ANALYSIS OF LOW-ENERGY DATA

Over a sufficiently limited range of energies, it is possible to parametrize simply the energy dependence of partial-wave amplitudes. Fortunately, also, experimental data from one group (Berkeley)⁸ are available at eight different momenta from 140 to 642 MeV/c. Although the start of the inelastic threshold corresponds to a beam momentum of 521 MeV/c, the inelastic cross section at 642 MeV/c is less than 0.5%,⁸ so that the data at all these momenta can be treated as being fully elastic. Furthermore, apart from the inelastic branch cut which we neglect, and possible singularities on the "second sheet" of the partial-wave amplitude, the function $M_l(k^2) = (k/\mu)^{2l} k \cos \delta_l$ is analytic in the k^2 plane except for a cut $-\infty < k^2 < -\mu^2$, so that one can make an effective range expansion

$$(k/\mu)^{2l} k \cot \delta_l = a_l^{-1} + \frac{1}{2} r_{0l} k^2 + \dots \quad (8)$$

This expansion, however, does not converge outside the circle $|k^2| \leq \mu^2$. One can increase the region of convergence by constructing the "parabolic" variable discussed in our earlier paper,²

$$p^2 = \mu^2 [\cosh^{-1}(1 + k^2/\mu^2)^{1/2}]^2, \quad (9)$$

and expanding $M_l(k^2)$ as

$$M_l(k^2) = a_l^{-1} + \frac{1}{2} r_{0l} p^2 + \dots \quad (10)$$

This variable transforms the left-hand cut to a parabola, and the Taylor expansion (10) is convergent for $|p^2| < \frac{1}{4}\pi^2\mu^2$, i.e., $(k^2)_{\max} \approx 5\mu^2$. (Considered as an expansion in orthogonal polynomials, the region of convergence is larger.)

Thus the expansion (10) was used to parametrize the partial-wave amplitudes. (LMO expand the phase shifts themselves as a power series.) In practice, the expansion (10) was used only for the large S -wave amplitudes in this low-energy region.

A preliminary analysis⁴ had indicated that even at $P_{\text{lab}} = 520$ MeV/c, the $P_{1/2}$ phases are too large to be ignored. Since one also wishes to consider the Fermi-Yang ambiguity, one is led to introduce at least three partial waves, $S_{1/2}$, $P_{1/2}$, and $P_{3/2}$, which is also the minimum number required for our transformation method to affect the analysis. The $P_{1/2}$ and $P_{3/2}$ phases are quite small, and a simple scattering length was found to be enough to characterize them. (Introduction of quadratic terms in S waves and/or linear

TABLE IV. Phase shifts (in degrees) obtained in energy-independent analyses at the laboratory momentum indicated (in MeV/c). In addition to the solutions listed, two distinct Y -type solutions were found at 1450 MeV/c.

P (lab)	(DF)	g^2		$-\frac{1}{2}$	$+\frac{1}{2}$	$+\frac{3}{2}$	$-\frac{3}{2}$	$-\frac{5}{2}$	χ^2						
(F)															
778	(18)	0	δ	-42.9	0.38	+0.66	-0.21	0.11	16.1						
			η	0.997	1.00	0.987	1.00	0.998							
		7	δ	-42.3	-3.0	2.3	-0.80	-0.80		15.3					
			η	1.00	0.999	0.987	0.998	0.998							
		14	δ	-39.6	-10.3	6.64	-0.85	-1.66			15.7				
			η	1.00	0.973	1.00	0.997	0.999							
		21	δ	-36.8	-15.0	9.0	-0.75	-2.6				20			
			η	0.999	0.990	1.00	0.994	0.998							
		860	(32)	0	δ	-48.3	-2.74	5.45					-5.43	0.94	25
					η	0.93	0.97	0.989					1.00	0.996	
7	δ			-49.0	-6.3	7.3	-4.9	0.48	22						
	η			0.82	0.89	0.84	1.00	0.996							
14	δ			-41.3	-11.7	11.5	-3.8	-1.6		21					
	η			0.999	0.966	0.986	0.995	0.988							
21	δ			-42.5	-13.9	10.9	-3.4	-3.4			25				
	η			0.93	0.991	0.993	0.996	0.996							
910	(10)			0	δ	-60.7	-8.0	2.9				-3.7	0.51	5.4	
					η	0.68	1.00	1.00				1.00	1.00		
		7	δ	-41.0	-14.2	10.5	-2.0	-0.2				5.1			
			η	1.00	0.87	0.98	0.988	0.985							
		14	δ	-31.8	-24.4	+15.6	-2.9	-1.4	4.3						
			η	1.00	0.68	0.976	0.979	0.975							
		21	δ	-26.0	-28.5	16.6	-4.0	-3.2		4.0					
			η	0.89	0.999	1.00	0.983	0.979							
		960	(38)	0	δ	-46.9	-8.14	10.1			-5.25		1.64		33
					η	0.997	0.91	0.91			0.993		0.978		
7	δ			-49.2	-9.44	8.33	-3.72	-0.88			32				
	η			0.983	0.943	0.91	0.988	0.980							
14	δ			-43.7	-19.5	10.9	-2.9	-2.5				33			
	η			0.96	0.68	0.999	0.993	0.992							
21	δ			-42.8	-22.7	13.1	-3.6	-4.1	37						
	η			0.82	0.86	0.999	0.980	0.999							
1170	(13)			0	δ	-43.9	-30.5	4.7		-8.6			0.22	15.8	
					η	0.88	0.29	0.79		1.00			0.96		
		7	δ	-45.9	-23.4	3.0	-8.0	-0.39		15.7					
			η	0.90	0.27	0.79	1.00	0.96							
		14	δ	-43.7	-24.9	1.5	-6.2	-1.0			15.8				
			η	0.981	0.22	0.78	0.983	0.96							
		21	δ	-34.7	-35.0	10.6	-5.8	-1.9				16.0			
			η	0.990	0.77	0.710	0.960	0.94							
		1200	(56)	0	δ	-32.5	-74.4	-3.0	-9.0				-1.1		84
					η	0.61	0.44	0.86	1.00				0.970		
7	δ			-35.1	-77.9	-5.0	-6.5	-1.3	82						
	η			0.72	0.37	0.85	0.995	0.971							
14	δ			-45.8	-30.1	6.2	-3.2	-3.4		82					
	η			0.92	0.81	0.89	0.95	0.95							
21	δ			-46.3	-32.3	6.8	-3.3	-4.0			82				
	η			0.82	0.83	0.74	0.96	0.96							

TABLE IV (Continued)

P (lab)	(DF)	g^2		$-\frac{1}{2}$	$+\frac{1}{2}$	$+\frac{3}{2}$	$-\frac{3}{2}$	$-\frac{5}{2}$	χ^2	
1450	(34)	0	δ	-46.3	-65.8	-11.2	-9.0	-4.9	47.5	
			η	0.48	0.35	0.76	0.993	0.96		
	7	δ	-43.4	-64.7	-11.4	-7.6	-5.7	48.7		
		η	0.46	0.42	0.70	0.980	0.96			
	14	δ	-41.5	-60	-11.2	-5.2	-7.5	49.7		
		η	0.39	0.26	0.82	0.94	0.999			
	21	δ	-43.7	-40.0	0.3	-8.3	-6.0	51.0		
		η	0.46	0.98	0.59	0.96	0.95			
	(Y)									
	860	(32)	0	δ	-47.3	6.0	-0.2	-4.3	0.002	33
η				0.90	0.86	0.997	1.00	0.999		
7		δ	-47.0	9.3	-0.6	-2.7	-1.9	30		
		η	0.990	0.86	0.999	1.00	1.00			
14		δ	-37.6	26.7	-4.3	-2.2	-4.2	22		
		η	0.998	0.978	0.96	0.993	1.00			
21		δ	-22.5	40.3	-5.2	-3.2	-6.0	22		
		η	0.973	0.89	0.998	1.00	1.00			
960		(38)	0	δ	-49.9	16.1	-4.8	-4.9	-0.8	44
				η	0.93	0.85	0.94	1.00	0.99	
	7	δ	-54.7	17.1	-3.0	-4.2	-2.7	37		
		η	0.81	0.75	0.99	1.00	0.99			
	14	δ	-46.6	20.0	-0.6	2.0	-4.5	32		
		η	0.98	0.70	0.96	0.99	1.00			
	21	δ	-46.9	19.4	-0.7	6.4	-6.4	38		
		η	0.89	0.75	0.97	1.00	1.00			
	1170	(13)	0	δ	-42.8	33.5	-4.4	1.6	-6.7	15.7
				η	0.90	0.22	0.79	0.96	0.988	
7		δ	-45.4	19.3	-3.3	0.9	-6.5	15.8		
		η	0.92	0.18	0.81	0.96	0.990			
14		δ	-42.1	26.6	-3.5	+0.3	-5.6	16		
		η	0.95	0.08	0.79	0.96	0.98			
21		δ	-40.0	34.6	-9.3	-3.2	-4.0	17		
		η	0.995	0.08	0.998	0.999	0.988			
1200		(56)	0	δ	-29.6	80.5	-8.4	1.4	-9.4	83.5
				η	0.51	0.37	0.89	0.97	1.00	
	7	δ	-31.0	83.3	-7.6	1.3	-9.5	83		
		η	0.48	0.35	0.90	0.976	1.00			
	14	δ	-35.5	83.8	-7.8	-2.3	-5.2	82		
		η	0.67	0.24	0.87	0.98	0.98			
	21	δ	-40.1	25.0	-17.9	-3.4	-2.7	84		
		η	0.989	0.67	0.81	0.95	0.94			

terms in $P_{1/2}$ and/or $P_{3/2}$ waves improves somewhat the fit at 642 MeV/c.) Thus we used four parameters to fit the 53 data points of Goldhaber *et al.*⁸ [There are 45 data on differential scattering cross sections and eight values of the real part of the forward amplitude taken from the dispersion relations^{19,20} (with large uncertainties).]

Our results are shown in Tables I and II. For the solution of the type F [$\delta(p_{1/2}) < \delta(p_{3/2})$], we find that the χ^2 is quite independent of g^2 in the range of in-

terest (one notes, however, the different phases obtained at 520 and 642 MeV/c for $g^2=0$ and $g^2 \neq 0$). For the solution of type Y [$\delta(p_{1/2}) > \delta(p_{3/2})$], we find that the best fit is obtained for $g^2 \lesssim 7$. Previous analysis⁷ and our analysis at higher momenta indicate that $g^2 \gtrsim 7$, which leads us to believe that for the favored solution in the low-energy region, $\delta(p_{1/2}) < \delta(p_{3/2})$. [If one considers only values of g^2 which are consistent with $SU(3)$, this F solution is the only acceptable one.] This favored solution is included in

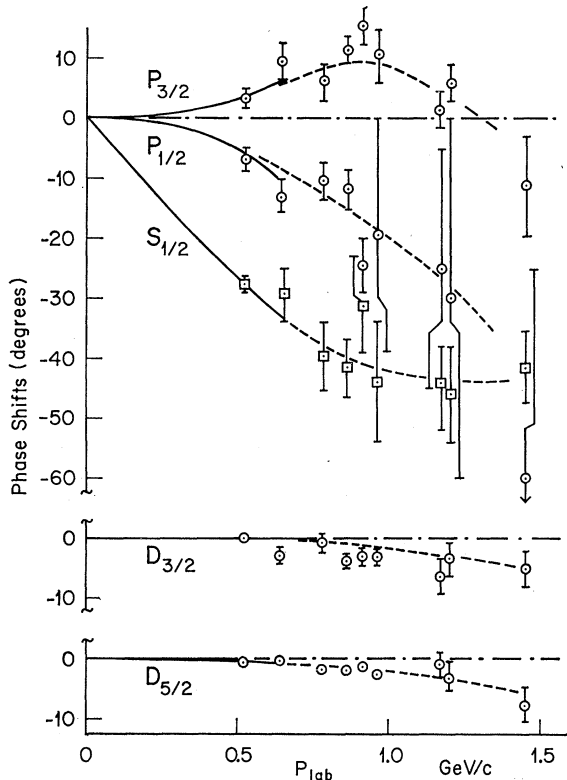


FIG. 1. Momentum dependence of the phase shifts. The S -wave points are denoted by squares. The energy-dependent fit of Sec. IV is shown as solid curves; a guess as to the continuation through the independent fits at higher single energies is shown by the dashed curves. The D -wave points shown as circles without error bars were not associated with adjustable parameters, but were generated from the more central partial waves. In obtaining all of the points on these curves, it was assumed that $g^2 = g_{KN\Lambda}^2 + g_{KN\Sigma}^2 = 14$.

Fig. 1. The only point which prevents us from getting a nearly exact fit is the most forward point at 205 MeV/c. We have, however, not retouched the data and have analyzed them as they were obtained from the published figures. Goldhaber *et al.*⁸ made an analysis with S waves only, and LMO a fit with smaller P waves. However, our fit is really very similar to theirs, except for small details.

Using expression (10) one can calculate the three phase shifts for 600 MeV/c. An estimate of the phases at this beam momentum (including charge-exchange data) has also been obtained by Ray *et al.*³ The agreement from two such widely different analyses, as shown in Table III, makes us believe that the phases found are approximately correct.

V. SINGLE-ENERGY ANALYSES

A. Low-Energy Data

There are data on the differential scattering cross section at 522 MeV/c by Kycia *et al.*⁹ We did not introduce this set in the above, in order to avoid

confusion by systematic errors. We did, however, make an analysis at this energy alone, and the phases obtained are shown in Fig. 1, and the fit in Fig. 2. To compare further the energy-dependent and energy-independent analyses, we compared the results also at 640 MeV/c. These results are also shown in Figs. 1 and 2. A small change in the P -wave amplitudes of 640 MeV/c would remove the small disagreement between the two fits.

B. 780 and 910 MeV/c

1. 780 MeV/c. From the experiments of Focardi *et al.*,¹⁰ data with very good statistics on differential scattering cross sections are available at 780-MeV/c lab momenta. The inelastic cross section is not negligible, and the total cross section is quite accurately known. There is also a measurement of polarization with large errors by Femino *et al.*¹¹ We carried out a very detailed search for all acceptable fits. It was found convenient to search for the real and imaginary parts of the partial-wave amplitudes instead of the phase shifts and the inelasticities. Since the ellipse of

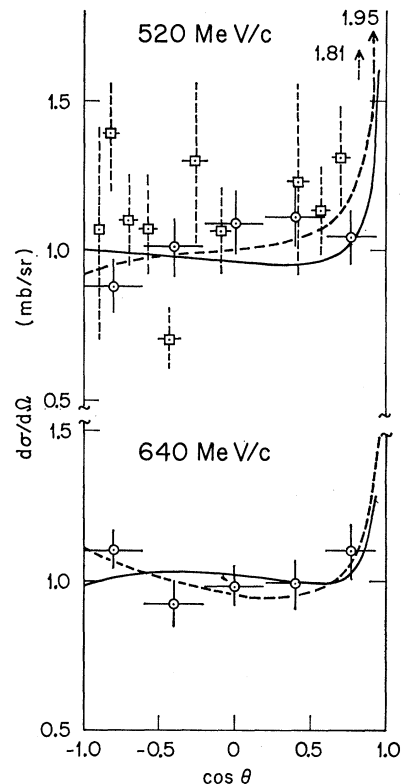


FIG. 2. Fits to the 520- and 640-MeV/c data. The circles denote the data of Goldhaber *et al.* (Ref. 8) and the squares denote the renormalized data of Kycia *et al.* (Ref. 9). The solid lines show the results of an energy-dependent fit including the lower-energy data of Goldhaber *et al.*, and the dashed lines show the best three-parameter energy-independent fits with $\delta(p_{1/2}) > \delta(p_{3/2})$. For all these fits, it was assumed that $g^2 = 14$.

convergence is larger for the imaginary part, a smaller number of parameters is needed for good fits to it. So we studied the solutions as they were obtained by searching on three real and three imaginary amplitudes and also on four real and three imaginary amplitudes. The best set of phases was again with $\delta(p_{1/2}) < 0$, and the results are shown in Table IV. The fit to the angular distribution is shown in Fig. 3. For comparison with our results, we also show the best fits to the differential cross-section data as obtained by the group of Focardi *et al.*¹⁰ using the standard method. It is evident from Fig. 3 that the inclusion of partial-wave amplitudes with $l \geq 2$ is required for an acceptable fit to the data; it is also quite clear that these amplitudes are required only in the amount by which they are automatically generated by our prescription.

Since the data had good statistics, we also studied the variation of χ^2 with g^2 , which is not inconsistent with other determinations (see Fig. 4). Furthermore, we note that consistency with the lower-energy fits requires $7 \lesssim g^2 \lesssim 21$.

2. 910 MeV/c. Hirsch and Gidal¹³ carried out measurements of the differential cross section at 910 MeV/c and also measured the polarization. The errors are so large that the resulting phase shifts have only qualitative significance; however, the $\delta(p_{1/2}) > 0$ solution is not obtained and furthermore, the fit is sensitive to g^2 . We again made a detailed study with six and seven parameters; the results are shown in Table IV, and a graph showing the variation of χ^2 with g^2 is given in Fig. 4.

At these two energies there is no Fermi-Yang ambiguity, so one can, with some confidence, assert that $\delta(p_{1/2}) < 0$, at least up to 910 MeV/c.

C. 860 and 960 MeV/c

These data from Berkeley¹² can be well fitted by seven parameters, the real parts of the ($S_{1/2}$, $P_{1/2}$,

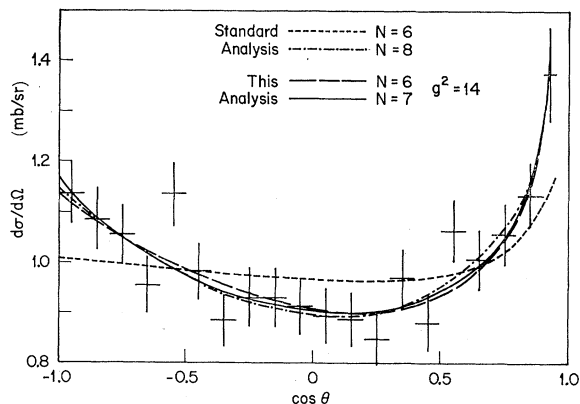


FIG. 3. Fits to the 778-MeV/c data of Focardi *et al.* (Ref. 10) using $g^2=14$. The "standard analysis" curves (Ref. 10) were fitted to the differential cross section and total inelastic cross section; for $N=6$, only S and $P_{1/2}$ waves were considered, while for $N=8$ elastic D waves were also included.

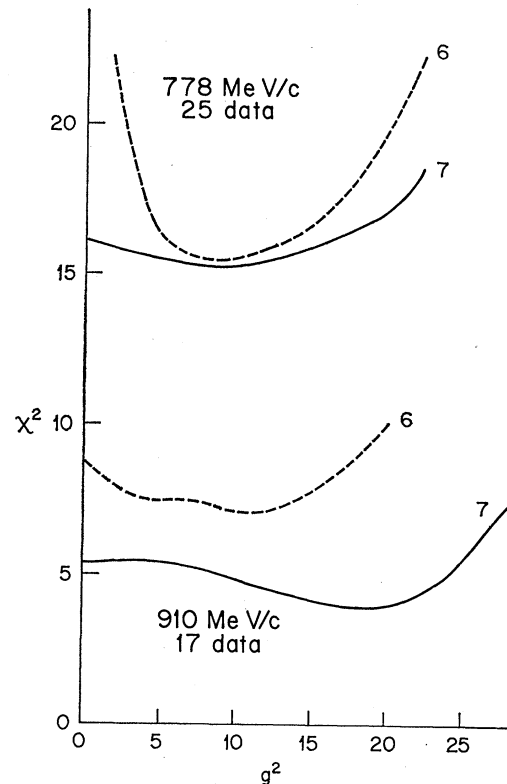


FIG. 4. Graphs illustrating the degree of sensitivity to the coupling-constant combination $g^2 = g_{KN\Lambda}^2 + g_{NK\Sigma}^2$, for two energies where polarization information existed before this work was carried out.

$P_{3/2}$, $D_{3/2}$) amplitudes, and the imaginary parts of the first three. They exhibit clearly two solutions (F and Y solutions) for all values of $g_A^2 + g_Z^2$, in the range 0–21. These solutions are tabulated in Tables IV and V. However, the analysis at 780 and 910 MeV/c having required that $\delta(p_{1/2}) < 0$, the solution for 860 MeV/c would still be $\delta(p_{1/2}) < 0$. At 960 MeV/c, however, besides the smoothly increasing $-\delta(p_{1/2})$, one could think of a $P_{1/2}$ -wave phase shift approaching zero or crossing over to the $\delta(p_{1/2}) > 0$ solution. Polarization data would greatly reduce the uncertainties in the phase shifts.

D. 1170 and 1200 MeV/c

The set at 1170 MeV/c consists of rather old (1961) spark-chamber data of Cook *et al.*¹⁴ but contains measurements close to forward angles. The set used at 1200 MeV/c was the Berkeley data¹¹ of 1967–1968 in our initial runs. We found first that both sets could be well fitted by seven parameters, as for the smaller (860, 960) beam momenta. We had, however, noted that even though the beam momenta are close, a combined analysis of both sets of data at an average momentum of 1190 MeV/c could not be fitted by seven parameters. When we included the recent BNL data¹⁵ at backward angles (we obtained a $\chi^2=95$ for

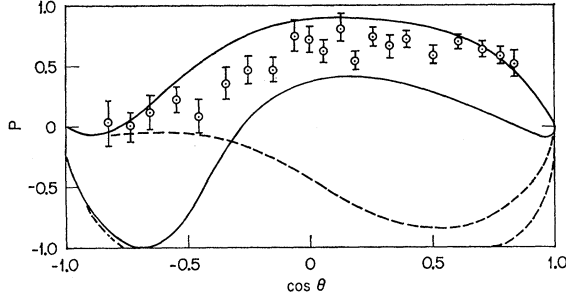


FIG. 5. The renormalized polarization data at 1220 MeV/c, compared with the predicted polarization at 1170 MeV/c (with $g^2=14$). The solid curves indicate, roughly, a one-standard-deviation band around the best fit with $\delta(p_{1/2}) < \delta(p_{3/2})$. The dashed curves (and the lower bound $P \geq -1$) gives the same information for the fits with $\delta(p_{1/2}) > \delta(p_{3/2})$. By comparing the size of the band with the error bars on the data, some idea can be gained of how the precision of the phase-shift determination can be increased by use of polarization data.

60 degrees of freedom), we also could not obtain a good fit with seven parameters at 1200 MeV/c alone. A somewhat more acceptable fit was obtained with eight parameters with five real amplitudes ($S_{1/2}$, $P_{1/2}$, $P_{3/2}$, $D_{3/2}$, and $D_{5/2}$) and the imaginary parts of the first three, the χ^2 dropping down to 80. It may be noted that after renormalization, the BNL data can form a good continuation of the 1170-MeV/c data.

With eight parameters we obtained two main solutions when only the 1200 MeV/c angular distribution data was used; these are shown in Tables IV and V. The polarization data of Andersson *et al.*¹⁴ are consistent with the solution shown in Table IV.

In view of the fact that systematic errors have been discovered in the 1200 MeV/c data,¹⁸ the results quoted for this set are not very significant. In this energy region, we found from the angular distribution what can be described as a two-parameter family of solutions; the two parameters can conveniently be taken as the real and imaginary parts of the $P_{1/2}$ amplitude, which could vary within wide limits, but with the other amplitudes then being strongly correlated with it. The polarization data essentially fix these parameters.

In Fig. 5 we have superposed the renormalized 1200-MeV/c polarization data on the bands of predicted polarizations obtained from the 1170-MeV/c differential cross section. The bands were obtained as the envelope of the polarization curves derived from constrained fits, when the $P_{1/2}$ amplitude was fixed at various points along the $\Delta\chi^2=1$ contour.

E. 1450 MeV/c

This set of data from CERN¹⁶ can be equally well fitted with seven or eight parameters, but the results quoted in the tables are for eight. At this momentum, all phases are negative, as are all the larger Born waves.

VI. SUMMARY

The primary results of this study are contained in the tables, especially Tables IV and V, and also in Fig. 1, which shows the trend with energy of the phase shifts obtained by the analysis reported here.

The uncertainties in the phase shifts, listed separately in Table V, are essentially independent of g^2 . However, we wish to remark that a realistic estimate of the uncertainty is very hard to obtain, because the χ^2 surface is quite irregular, as is common in this sort of work. The inelasticity parameters η are all uncertain by about 50% of the amount by which they differ from unity.

However, our motivation in undertaking this work was only in part derived from the desire to clarify the nature of K^+p interactions. We also had the aim of testing our proposed new method for partial-wave analysis in a practical application and, in particular, to see whether any unexpected technical problems would impair its usefulness. Compared with the usual partial-wave expansion, the one used here has strong theoretical advantages. It has sometimes been considered that the ordinary expansion is the simplest and easiest to use. However, our experience in this work has shown that the improved expansion is just as convenient, when organized in the manner described in Sec. II; thus, the traditional method has no advantages whatsoever, which could compensate for its inherent biases.

A perhaps unexpected bonus of our new method is that fewer ambiguous sets of fits were obtained. This was also noted by Ray *et al.*³ In addition, we did not need to make any arbitrary guesses about which partial waves were responsible for the inelasticity.

A question of great interest at the time this work was begun concerned the existence of a $P_{1/2}$ resonance. The data of Andersson *et al.*⁴ proved that this suspected resonance did not exist, although, indeed, our fits at lower energies also definitely favored the non-resonant possibility. The question of a resonance in the $P_{3/2}$ partial wave is still open. However, we wish to point out that the possible counterclockwise motion in the Argand diagram might be associated not

TABLE V. Uncertainties for the phase shifts obtained with $g^2=14$ listed in Table IV (F). These may be considered typical. The uncertainty in $(1-\eta)$ is about 50%.

$P(\text{lab})$	$-\frac{1}{2}$	$+\frac{1}{2}$	$+\frac{3}{2}$	$-\frac{3}{2}$	$-\frac{5}{2}$
780	6	2.5	3	1.5	...
860	5	3	2.5	1	...
910	8	4	3	1.5	...
960	10	20	3.5	1.5	...
1170	7	20	3	3	2
1200	8	30	3	2	3
1450	6	35	8	3	3

with a resonance pole on the unphysical sheet, but instead with the complex normal threshold branch cuts for the two-body processes $K+N \rightarrow K+\Delta$ or $K+N \rightarrow K^*+N$. Very precise data and careful analysis would be required to distinguish between a pole and a branch cut.

Finally we wish to emphasize that, apart from the importance for establishing the trends of the phase shifts, highly accurate data on the differential scattering cross section and polarization in this energy

region would be especially valuable, in that they would make possible a precision determination of the coupling constants.

ACKNOWLEDGMENTS

We wish to thank Y. A. Chao, Professor A. Engler, Dr. H. E. Fisk, Dr. R. Kraemer, and Dr. A. Ray (C-MU), as well as Dr. A. T. Lea, Dr. B. R. Martin, and Dr. G. C. Oades (Rutherford Laboratory) for interesting and useful discussions.

Inelastic Processes in the Eikonal Expansion*

ROBERT A. RUDIN†

Physics Department, Rutgers-The State University, New Brunswick, New Jersey 08903

(Received 18 November 1969)

Glauber's eikonal approximation for multiple scattering is extended to include inelastic processes. It is found that inelastic contributions to the differential cross section for the reaction $\pi^-d \rightarrow \pi^-d$ are negligible, while such contributions dominate the double-charge-exchange reaction $\pi^-He^3 \rightarrow \pi^+3n$.

I. INTRODUCTION

THE systematic presentation made by Glauber of the high-energy eikonal approximation¹ has made possible the widespread use of this method in recent years to analyze high-energy scattering data. This method makes it possible to express the scattering amplitude for the process of an elementary projectile incident on a composite target in terms of the elastic amplitudes for the same projectile incident on the individual constituents of the target, and of certain parameters of the target. The approximation has thus been used extensively in the analysis of hadron-hadron interactions at high energy and of nuclear-structure parameters.²⁻¹⁶ Until recently, however, very little of

this work has treated pion-nucleus interactions.^{8,9,17} Some work has been done on charge-exchange scattering, but only as quasi-elastic corrections to elastic processes.^{4,6,10,17}

If \mathbf{k} and \mathbf{k}' represent, respectively, the initial and final momentum of the projectile, formal derivation of the multiple-scattering expansion as it is commonly used requires that \mathbf{k} be nearly perpendicular to $\mathbf{k}-\mathbf{k}'$ for small scattering angles.^{1,2} This condition is met for elastic and quasi-elastic (e.g., $\pi^-p \rightarrow \pi^0n$) processes, but is invalidated by the longitudinal momentum transfer involved in inelastic processes (e.g., $\pi^-p \rightarrow \rho^0n$). Attempts have been made to modify this approximation to include such processes,^{12,13} but we feel that the present analysis is considerably more transparent.

In this paper we rigorously extend the eikonal approximation to include inelastic processes in order to understand better all contributions to a given reaction, and we note one process in particular which could provide a test of the theory as well as an excellent vehicle for the study of certain resonances.

We begin in Sec. II with a reformulation of the multiple-scattering expansion in terms of coupled channels of different mass. The resulting expression reduces to the Glauber result in the special case of elastic scattering or channels of equal mass, but takes specific account of the longitudinal momentum transfer in the unequal-mass case.

Section III contains a brief study of the reaction $\pi^-d \rightarrow \pi^-d$, paying particular attention to inelastic intermediate-state contributions. Section IV is an analysis of the double-charge-exchange reaction $\pi^-He^3 \rightarrow \pi^+3n$. It is shown that inelastic processes

* Portions of this work were completed while the author was a NASA Predoctoral trainee, and portions while a National Science Foundation Predoctoral Trainee.

† Present address: Physics Department, The Cooper Union, Cooper Square, New York, N.Y. 10003.

¹ R. J. Glauber, *Lectures in Theoretical Physics* (Interscience, New York, 1959), p. 315.

² D. Harrington, *Phys. Rev.* **135**, B358 (1964).

³ V. Franco and R. J. Glauber, *Phys. Rev.* **142**, 1195 (1966).

⁴ V. Franco and E. Coleman, *Phys. Rev. Letters* **17**, 827 (1966).

⁵ R. H. Bassel and C. Wilkin, *Phys. Rev. Letters* **18**, 871 (1967).

⁶ R. J. Glauber and V. Franco, *Phys. Rev.* **156**, 1685 (1967).

⁷ W. Czyz and L. Lesniak, *Phys. Letters* **24B**, 227 (1967); **25B**, 319 (1967).

⁸ H. C. Hsiung, E. Coleman, B. Roe, D. Sinclair, and J. Vander Velde, *Phys. Rev. Letters* **21**, 187 (1968).

⁹ J. C. Vander Velde, University of Michigan Report, 1968 (unpublished).

¹⁰ C. Wilkin, *Phys. Rev. Letters* **17**, 561 (1966).

¹¹ E. Kujawski, D. Sachs, and J. Trefil, *Phys. Rev. Letters* **21**, 583 (1968).

¹² J. Formánek and J. S. Trefil, *Nucl. Phys.* **B3**, 155 (1967).

¹³ J. S. Trefil, *Phys. Rev.* **180**, 1366 (1969); M. Ross and L. Stodolsky, *ibid.* **149**, 1172 (1966).

¹⁴ W. Czyz and L. C. Maximon, *Phys. Letters* **27B**, 354 (1968).

¹⁵ R. J. Glauber, *High Energy Physics and Nuclear Structure* (North-Holland, Amsterdam, 1967), p. 311.

¹⁶ R. H. Bassel and C. Wilkin, *Phys. Rev.* **174**, 1179 (1968).

¹⁷ C. Michael and C. Wilkin, *Nucl. Phys.* **B11**, 99 (1969).